Journal of Materials Chemistry B

Accepted Manuscript

ROYAL SOCIETY OF CHEMISTRY

www.rsc.org/materialsB

Cite this: DOI: 10.1039/c0xx00000x

www.rsc.org/xxxxxx

ARTICLE TYPE

Three-dimensional Amylopectin-Reduced Graphene Oxide Framework for Efficient Adsorption and Removal of Hemoglobin

Yue Zhang, Jia-wei Liu, Xu-wei Chen* and Jian-hua Wang*

Received (in XXX, XXX) Xth XXXXXXXXX 20XX, Accepted Xth XXXXXXXXX 20XX

DOI: 10.1039/b000000x

A three-dimensional graphene oxide framework is prepared via a simple and cost-effective one-pot approach through the hydrogen-bonding interaction between amylopectin and graphene oxide in the presence of hydrazine hydrate acting as reducing reagent. The framework is shortly termed as AP-rGO and it is characterized by Fourier transform infrared spectroscopy (FT-IR), scanning electron microscopy (SEM), surface charge analysis and thermogravimetric analysis (TGA). The obtained AP-rGO framework exhibits excellent adsorption performance toward hemoglobin in the presence of other protein species. It provides a maximum adsorption capacity of 1010 mg g^{-1}. In a neutral medium (at pH 7), 70 mg L^{-1} Hb in 1.0 mL of aqueous solution could be effectively adsorbed by 1.0 mg of the AP-rGO framework, giving rise to an adsorption efficiency of 92.7%. The practical application of the AP-rGO framework is demonstrated by the removal of high abundant protein, i.e., hemoglobin, from complex biological sample matrixes, e.g., human whole blood. The removal efficiency is well confirmed by sodium dodecyl sulfate polyacrylamide gel electrophoresis (SDS-PAGE) assay.

1. Introduction

As a kind of novel two-dimensional carbon material, graphene has attracted extensive attentions due to its specific physical and chemical properties. [1] Graphene oxide (GO) is the oxidized derivative of graphene and shows improved reaction activities and biocompatibility due to the abundant oxygen-containing functional groups on the surface. During the last decade, GO and its derivatives have been widely employed in various fields, e.g., energy storage, [2] biosensor, [3] cell imaging [4] and drug delivery. [5] Recently, it has been demonstrated that GO could mimic protein-protein interface, which might induce favorable adsorption of protein species onto GO surface. [6] However, the abundant hydrophilic groups on GO surface make it highly dispersive in aqueous medium and it is thus quite difficult to achieve effective separation of GO from the reaction medium after the process of adsorption. It is even not feasible with high speed centrifugation or filtration process. This is an obvious limitation for the direct utilization of GO in the field of bio-separation. In this respect, modification of GO or its assembly onto suitable solid support via covalent or non-covalent functionalization approach has been proved to be an efficient strategy for this purpose. [7-10] Generally, part of the binding sites on GO surface are occupied by certain functional groups during the modification or assembly process, and thus results in a loss of adsorption capacity. Recently, it has been demonstrated that three-dimensional (3D) GO/rGO materials not only possess the intrinsic properties of the 2D grapehene derivatives, but also provide advanced functions with improved performance in the fields of catalysis, [11,12] sensor [13] and energy storage. [14-16] In the field of separation, the biocompatible 3D GO/rGO materials with large specific surface area also exhibit favorable advantages and potential applications attributing to the much improved adsorption capacity and high efficiency as well as fast adsorption. [17,18] Meanwhile, the preparation of 3D GO/rGO based material is performed under rigorous experimental conditions, e.g., ultra-high temperature, and very often the sacrifice of template is inevitable.

Since the development of "Green Chemistry" in the last decades, [19] natural polymers have been paid increasing attentions because of their biodegradability, biocompatibility and renewability. [20] Amylopectin (AP) is one of the most attractive natural polymers composed of linear chains of (1->4)-α-D-glucose residues. It is usually employed for the accommodation of volumetric expansion due to its excellent aging resistance. [21] Generally, AP is semi-crystalline and insoluble in water at room temperature. When it is heated with excessive amount of water, the hydrogen bonds among AP molecules tend to break accompanied by the disruption of its crystalline structure, along with the formation of new hydrogen bonds between water molecules and the exposed hydroxyl groups of AP, which results in an increase on granule swelling and solubility. [22] This feature illustrates great potentials for AP as a precursor for the modification of certain materials and the improvement on their performance.

Herein, we report a simple and cost-effective process for the preparation of three-dimensional AP-rGO composite framework through hydrogen-bonding interactions between the amylopectin chain and graphene oxide in the presence of hydrazine hydrate acting as reducing reagent. The produced 3D AP-rGO composite framework exhibits a super-high adsorption capacity toward hemoglobin, along with favorable adsorption selectivity under

controlled experimental conditions (at pH 7 in 4.0 mmol L^{-1} Britton-Robinson buffer solution). It thus offers a promising medium for the exploitation of high abundance protein removal from biological sample matrixes, in this particular case, the removal of hemoglobin from human whole blood.

2. Materials and Methods

2.1. Materials and reagents

Amylopectin (AP, from waxy maize, 99.7%, Derui Bio-techology Co. Ltd, Zhengzhou, China), hydrazine hydrate (85%, w/w, Sinopharm Chemical Reagent Co. Ltd, Shanghai, China) and high purity graphite powder (Sinopharm Chemical Reagent Co. Ltd, Shanghai, China) are employed as received. Other reagents employed including H_2SO_4, $K_2S_2O_8$, P_2O_5, H_3BO_4, $NaNO_3$, $KMnO_4$, H_2O_2 and HCl are obtained from Bodi Chemical Holding Co. Ltd. (Tianjin, China) and at least of analytical reagent grade. Deionized water is used throughout.

Bovine serum albumin (BSA, A 3311, >98%) is purchased from Sigma-Aldrich (St. Louis, USA) and hemoglobin from bovine blood (Hb, 95%) is obtained from Sinopharm Chemical Reagent Co. Ltd (Shanghai, China). These proteins are used without further purification. The protein molecular weight marker (broad, D532A, Takara Biotechnology Company, Dalian, China) is a mixture of nine purified proteins (Mr in kDa: myosin, 200; β-galactosidase, 116; phosphorylase B, 97.2; serum albumin, 66.4; ovalbumin, 44.3; carbonic anhydrase, 29; trypsin inhibitor, 20.1; lysozyme, 14.3; aprotinin, 6.5). Human whole blood samples of healthy volunteers are provided by the Hospital of Northeastern University. All experiments were performed in compliance with the relevant laws and institutional guidelines with the use of human subjects, under the supervision of the Academic Ethics Committee of the University.

2.2. Preparation of the AP-rGO composite framework

GO is firstly synthesized according to the Hummers' method. [23, 24] 30 mL of homogeneous GO aqueous suspension (1.0 mg mL^{-1}) is obtained by mild sonication for 4 h. 1.0 g of AP powder is then added into the above suspension with a AP/GO mass ratio of 100/3. Thereafter, 30 mL of dimethyl sulfoxide (DMSO) is added to dissolve the AP powder and 90 μL of hydrazine hydrate is added as reducing agent for the conversion of GO into rGO. The mixture is heated and refluxed under magnetic stirring at 95 °C for 24 h. Afterwards, the black product is filtered with 1.2 μm cellulose membrane and washed by deionized water for five times to remove any residual DMSO. Finally, the obtained AP-rGO composite framework is freeze-dried under vacuum for 12 h and collected for further use.

2.3. Characterization of the AP-rGO composite framework

The surface morphologies of AP, rGO and AP-rGO composite framework were recorded on a S-3400N scanning electron microscope (SEM, Hitachi High Technologies, Japan). Fourier transform infrared (FT-IR) spectra of GO, rGO, AP and AP-rGO were measured by a Nicolet 6700 spectrometer (Thermo Electron, USA) from 400 to 4000 cm^{-1}. The surface charge properties of GO, rGO and AP-rGO in aqueous solution within pH 4-11 were measured by a ZEN3600 Nano Zetasizer (Malvern, UK). Nitrogen sorption-desorption isotherms are measured at −196 °C by a Micromeritcs Tristar 3000 analyzer (USA) at a relative pressure range from 0.05 to 0.25 for obtaining the specific surface area.The thermogravimetric analysis (TGA) is performed by a TGA/DSC 1 STAR^e System (Mettler-Toledo, Switzerland) from 30 °C to 500 °C with a heating rate of 10 °C min^{-1} under N_2 atmosphere.

2.4. Proteins adsorption with AP-rGO composite framework

In the present work, hemoglobin and bovine serum albumin were employed as model proteins and their adsorption behaviors onto the AP-rGO composite framework were carefully investigated in 4 mmol L^{-1} Britton-Robinson (B-R) buffer at pH 4-11.

Typically, 1.0 mg of AP-rGO composite framework and 1.0 mL of protein solution (70.0 mg L^{-1}) was added into a 1.5-mL centrifuge tube. The mixture was then shaken vigorously for 30 min to facilitate the adsorption of proteins onto the surface of AP-rGO composite. After centrifugation at 8000 rpm for 8 min, the supernatant is collected to quantify the residual protein concentration. The adsorption efficiency of proteins was calculated as described in the following equation, where C_0 and C_1 represent the protein concentrations in original solution and in the supernatant respectively, and E is the adsorption efficiency.

$$E = \frac{C_0 - C_1}{C_0} \times 100\%$$

3. Results and Discussion

3.1. Preparation and characterization of the AP-rGO composite framework

The one-pot preparation procedure for the AP-rGO composite framework is illustrated in Scheme 1. Upon heating at 95 °C, the hydrogen bonds among AP molecules tend to break and the dissolution of AP granules leads to the formation of homogenous hydrogel. [22] At the same time, new hydrogen bonds are formed between the oxygen-containing functional groups on GO and the hydroxyl groups on AP, which generates AP-GO cross-linking and eventually results in the formation of 3D AP-rGO composite framework. [21] During this preparation process, hydrazine hydrate is added as reducing reagent for the chemical reduction of GO and the formation of rGO. [25]

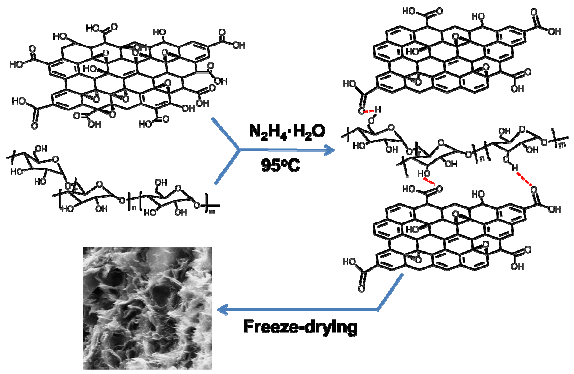

Scheme 1. The schematic illustration for the preparation of AP-rGO composite framework via the one-pot procedure.

Figure 1 shows the FT-IR spectra of GO, rGO, AP and AP-rGO composite framework. After GO is reduced to rGO by hydrazine, an obvious decrease on the intensity of absorption

bands at 3357 and 1731 cm^{-1} is observed, due to the reduced amount of -COOH groups. At the same time, the absorption band at 1619 cm^{-1} related to the bending vibration of O-H shifts to 1571 cm^{-1} due to the reduction of oxygen-containing groups on the surface of rGO sheets. [26] In the case of AP, the broad absorption band at 3357 cm^{-1} is contributed to the stretching vibration of the O-H and the absorption band at 1646 cm^{-1} is assigned to the O-H stretching vibration of water. After the formation of AP-rGO composite framework, a new absorption band at 1571 cm^{-1} is observed, corresponding to the O-H bending vibration of rGO. It is seen that the strong absorption band at 1020 cm^{-1} derived from the C-O-C stretching vibration become much stronger due to the introduction of rGO. In comparison with the FT-IR spectra of AP and rGO, an obvious blue shift from 3357 cm^{-1} to 3284 cm^{-1} is recorded for the AP-rGO composite framework for the absorption of O-H stretching vibration. This should be attributed to the formation of hydrogen bonds between the oxygen-containing functional groups of GO and the hydroxyl groups of AP, which induces the migration of electron cloud from O-H to O atom.

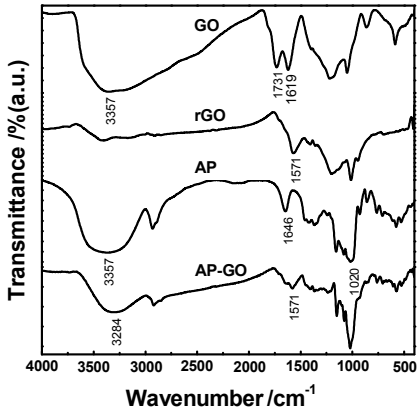

Figure 1. FT-IR spectra for GO, rGO, AP and AP-rGO composite framework.

The SEM images for AP, rGO and AP-rGO composite framework obtained under various AP/GO mass ratios are shown in Figure 2. It can be seen that AP granules are irregular shaped with smooth surface and their sizes are ranging from 2-30 μm (Figure 2A). In the case of rGO sheets, a lot of wrinkles are observed on its surface (Figure 2B). After formation of the AP-GO composite framework, the edges of 3D structure become more obvious with the increase of the mass ratio of AP/GO (Figure 2C-H). In this study, a AP/GO mass ratio of 100/3 is adopted and the AP-rGO composite framework originated from this mass ratio is used for the ensuing investigations.

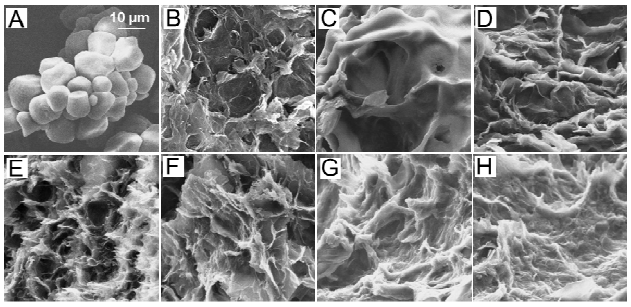

Figure 2. SEM images of the AP granules (A), rGO (B) and AP-rGO composite framework originated from various AP/rGO mass ratios: 100/1 (C); 100/2 (D); 100/3 (E); 100/4 (F); 100/5 (G); 100/10 (H).

The BET surface area of AP, rGO and AP-rGO composite are derived to be 0.543, 135.947 and 9.839 $m^2 g^{-1}$, respectively. It is clearly seen that the incorporation of GO into the AP-rGO composite significantly improves its specific surface area, which demonstrates the formation of 3D framework.

The thermogravimetric analysis results indicate that a remarkable weight loss at ca. 280 ^oC is observed for AP (Figure 3), which should be attributed to the pyrolysis of AP. A similar weight loss is also observed for the AP-rGO composite, while the weight loss in the latter case is much less than that for AP, due to the presence of rGO in the obtained composite framework. The oxygen-containing groups on rGO start to decompose at 130 ^oC. It is interesting to see that an increase of the decomposition temperature of rGO in AP-rGO composite is observed, i.e., within 130 ^oC to 160 ^oC, which might be contributed by the formed hydrogen bonds between rGO and AP. This observation is consistent with that reported in a literature that hydrogen bonding interactions between OH groups and rGO leads to improved thermal stability. [27]

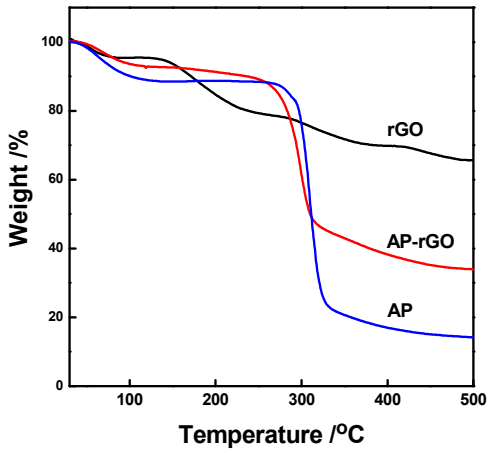

Figure 3. TGA analysis results for AP, rGO and AP-rGO composite framework.

3.2. Protein adsorption behavior by the AP-rGO composite framework

The adsorption behaviors of Hb and BSA by the AP, rGO and AP-rGO composite framework originated from various AP/rGO mass ratios are illustrated in Figure 4. The results clearly shown that rGO offers non-specific adsorption toward both Hb and BSA. On the contrast, in the presence of BSA, AP adsorbs Hb with favorable selectivity. However, only a limited adsorption efficiency of ca. 52% is achieved for Hb in this case. After the formation of AP-rGO composite framework, the adsorption efficiency for Hb is obviously improved up to 90.7% when the AP/rGO mass ratio is increased from 100/1 to 100/3, and meanwhile it maintains the selectivity against BSA, thereafter, a further increase of the AP/rGO mass ratio results in a gradual decrease of the adsorption efficiency for Hb. This might be due to the fact that the AP-rGO composite originated from a AP/rGO mass ratio of 100/3 provides a largest surface area as demonstrated in the SEM image in Figure 2E.

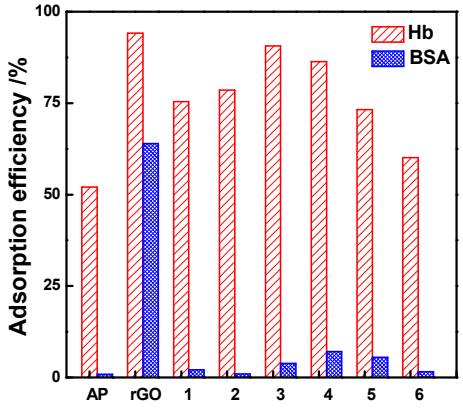

Figure 4. Adsorption efficiencies of Hb and BSA on AP, rGO and AP-rGO composite framework originated from various AP/rGO mass ratios (1-100/1, 2-100/2, 3-100/3, 4-100/4, 5-100/5, 6-100/10). Concentration/volume of protein solution: 70 mg L−1/1.0 mL; Amount of sorbent: 1.0 mg; Adsorption time: 30 min; pH 6.

The adsorption behaviors of Hb and BSA by AP, rGO and AP-rGO composite toward Hb and BSA are further investigated within pH 4-11, and the results are illustrated in Figure 5. As far as AP is concerned, a maximum adsorption for Hb is achieved at its isoelectric point, and meanwhile no BSA is adsorbed within the whole pH range investigated. It has been previously demonstrated that there are chemical interactions between the hydroxyl groups of polysaccharide and metal ions. [28] In the present case, the exposure of heme group in hemoglobin under neutral condition facilitates the coordination of hydroxyl groups of polysaccharide with the sixth vacant coordinating position of Fe^{2+} in the hemoglobin framework. This contributes to the favorable adsorption of hemoglobin at its isoelectric point. In an acidic medium, the protonation of hydroxyl groups of polysaccharide takes place which decreases its coordination with Fe^{2+}. On the other hand, in a basic medium the hydroxylation of Fe^{2+} blocks the binding of hydroxyl groups in the polysaccharide. [29] These results in the decrease of Hb adsorption as the pH value deviates from its isoelectric point. On the contrary, for the case of BSA there is no similar interaction involved as described for Hb, and thus no adsorption of BSA by AP is observed.

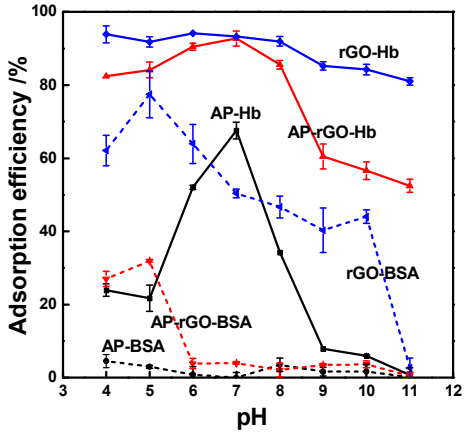

Figure 5. The pH-dependent adsorption of Hb and BSA by AP, rGO and AP-rGO composite framework (originated from a AP/rGO mass ratio of 100/3). Concentration/volume of protein solution: 70 mg L^{-1}/1.0 mL; Amount of sorbent: 1.0 mg; Adsorption time: 30 min.

Similar adsorption behaviors for Hb and BSA are observed by using rGO and AP-rGO composite framework as adsorbent. It is obvious that favorable adsorption for Hb and BSA is achieved at their isoelectric points by both adsorption media. At pH values around the isoelectric point of a specific protein, it becomes neutral and the hydrophobic residues are prone to exposure. It has been well documented that the aromatic groups of protein, e.g., tryptophan/tyrosine residues and the porphyrin rings of heme group, combine with the conjugate π-electron moieties of rGO via π-π stacking, [30, 31] leading to favorable adsorption. There are four heme groups in Hb structure and no heme group is involved in BSA, [32] the hydrophobic interaction between Hb and rGO is much stronger than that between BSA and rGO, resulting in favorable adsorption efficiency for Hb. This is in agreement with that achieved in a previous observation. [30]

The surface charge analysis results indicate that the surface of AP-rGO framework is negatively charged within the pH range studied. Therefore, electrostatic attraction between the AP-rGO composite and the positively charged hemoglobin provides an additional contribution to the adsorption of protein at pH≤pI. On the other hand, at pH higher than the isoelectric point the proteins turn into negatively charged, and thus the electrostatic repulsion leads to a decline for protein adsorption. It is seen that no adsorption of BSA is observed by the AP-rGO composite framework at pH > 6, while favorable adsorption of Hb is achieved within pH 6-8. This observation indicates that large percentage of AP involved in the process for the preparation of AP/rGO composite offers a favorable adsorption to Hb, and meanwhile the adsorption of BSA is greatly suppressed. Meanwhile, hydrophobic interactions between Hb and rGO further improved the adsorption of Hb. These eventually lead to the selective adsorption of Hb at pH 7 in the presence of other protein species, e.g., BSA in this case. An adsorption efficiency of 92.7% was achieved. For further studies, pH 7 is adopted for the sample solution and it is maintained by using a 4.0 mmol L^{-1} Britton-Robinson (B-R) buffer.

The influence of ionic strength on the adsorption of Hb is further investigated. The results indicated that the adsorption of Hb onto AP-rGO composite framework is virtually not affected by the variation of ionic strength at <0.7 mol L^{-1} NaCl. This observation suggested that electrostatic interaction is not among the main driving forces for Hb adsorption. That is, the adsorption

of Hb onto the AP-rGO composite framework is mainly governed by the hydrophobic interaction between Hb and AP-rGO composite, as well as the coordination of hydroxyl groups of polysaccharide in the AP moiety with Fe^{2+} in the hemoglobin framework.

3.3. Adsorption capacity for hemoglobin by the AP-rGO composite framework

The adsorption capacity of hemoglobin on the AP-rGO composite framework is investigated at room temperature within a concentration range of 10-550 μg mL^{-1} at pH 7. The experimental data are then fitted with the Langmuir adsorption model as expressed in the following. C^* and Q^* represent Hb concentration in the aqueous solution and the amount of Hb retained by the AP-rGO composite framework. Q_m is the maximum adsorption capacity and K_d denotes the dissociation constant.

$$Q^* = \frac{Q_m \times C^*}{K_d + C^*}$$

An ultra-high maximum adsorption capacity of 1010 mg g^{-1} Hb is derived by the AP-rGO composite framework. Table 1 summarizes a comparison of the adsorption capacities for hemoglobin by various adsorbents reported very recently. [30, 33-37] It is clearly seen that AP-rGO composite framework offers a much improved adsorption capacity for Hb due to its three-dimensional structure as well as the various interactions involved in the adsorption process. When considering GO-based adsorbents as described in the previous studies, [30, 37] AP-rGO composite framework provides a tremendous improvement on the sorption capability for hemoglobin, probably due to the change of surface property after reduction. The molecular flattening mechanism has indicated that the reduction of GO by hydrazine hydrate causes the formation of more sp^2 domains on its surface, [38,39] which facilitates the π–π stacking interactions between the heme group in the framework of hemoglobin and the rGO nanosheets involved in the AP-rGO composite framework.

Table 1. A comparison on the adsorption capacity of Hb by various adsorbents

Sorbents	Adsorption capacity (mg g^{-1})	Ref.
Cu^{2+} ion charged membrane	219.5	33
Imidazoliumm-polystyrene	23.6	34
Polymer-grafted Fe_3O_4 nanocellulose	248.2	35
Polydopamine-based molecular imprinting on Si-Fe_3O_4	4.6	36
GO on SiO_2	50.5	30
GO-MOFs	193.0	37
AP-rGO composite framework	1010.0	This work

3.4. Selective removal of hemoglobin from human whole blood

It is well known that hemoglobin is an abundant protein in human blood. For practical biological studies, it is highly desired to effectively and selectively remove hemoglobin in the presence of other protein species. In this respect, the AP-rGO composite framework is applied to the selective adsorption and removal of Hb from human whole blood. The human whole blood sample is diluted 100-fold by a 4.0 mmol L^{-1} B-R buffer solution. After centrifugation, the supernatant is collected for the adsorption and removal process. 250 μL of the above treated sample solution, 5 mg of AP-rGO composite and 750 μL of 4.0 mmol L^{-1} B-R buffer are sequentially added into a 1.5-mL centrifuge tube. The reaction mixture is shaken for 30 min followed by centrifugation at 8000 rpm. The supernatant is collected and employed for SDS-PAGE assay. As illustrated in Figure 6, clear bands of HSA and Hb are observed in the diluted human whole blood sample (Lane 2). After treatment by the AP-rGO composite, the band for Hb is completely disappeared while the band for HSA and its intensity remain unchanged (Lane 3). These results well suggest that Hb of high abundance in whole blood sample is selectively removed by the adsorption of AP-rGO composite. This illustrates the practical applicability of the novel composite framework in the removal of Hb from complex biological sample matrixes in the presence of other protein species.

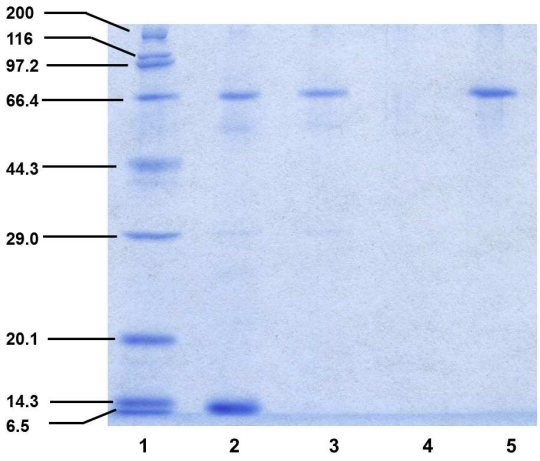

Figure 6. The SDS-PAGE assay results. Lane 1: Molecular weight standards (Marker in kDa); Lane 2: 400-fold diluted human whole blood; Lane 3: 400-fold diluted human whole blood after adsorption by the AP-rGO composite framework; Lane 4: blank; Lane 5: BSA standard solution of 100 mg L^{-1}.

4. Conclusions

Three-dimensional amylopectin (AP)-graphene oxide (GO) composite framework (shortly as AP-rGO) is derived via a simple and cost-effective one-pot approach through hydrogen-bonding interaction under reduction by hydrazine hydrate. The AP-rGO composite remains the abundant binding sites on GO surface and the adsorption property of AP to Hb, therefore, it exhibits a super high adsorption capacity towards Hb with respect to those reported in the literatures for various adsorbents. The present approach for developing a promising sorption medium for

hemoglobin provides a new avenue for future development of efficient adsorbents for specific target molecules.

Acknowledgements

The authors appreciate financial supports from the Natural Science Foundation of China (21275027, 21235001 and 21475017), the Program of New Century Excellent Talents in University (NCET-11-0071), Liaoning Provincial Natural Science Foundation (2014020041) and Fundamental Research Funds for the Central Universities (N110805001, N120605002, N120405004 and N130105002).

Notes and references

Research Center for Analytical Sciences, College of Sciences, Northeastern University, Shenyang, China. Fax: +86 24 83676698; Tel: +86 24 83688944; E-mail:chenxuwei@mail.neu.edu.cn (X.-W. Chen); jianhuajrz@mail.neu.edu.cn (J.-H Wang).

† Electronic Supplementary Information (ESI) available: Scheme for the preparation of DOX-GO-PEG-β-FeOOH nanocomposite; Conjugation of GO-PEG-β-FeOOH with RBITC; etc. See DOI: 10.1039/b000000x/

1. Y. Zhu, S. Murali, W. Cai, X. Li, J. W. Suk, J. R. Potts and R. S. Ruoff, *Adv. Mater.*, 2010, **22**, 3906.
2. V. Chabot, D. Higgins, A. Yu, X. Xiao, Z. Chen and J. Zhang, *Energy Environ. Sci.*, 2014, **7**, 1564.
3. C. Shan, H. Yang, J. Song, D. Han, A. Ivaska and L. Niu, *Anal. Chem.*, 2009, **81**, 2378.
4. T. Mosaiab, I. In and S. Y. Park, Macromol. *Rapid Commun.*, 2013, **34**, 1408.
5. M. L. Chen, Y. J. He, X. W. Chen and J. H. Wang, *Bioconjugate Chem.*, 2013, **24**, 387.
6. S. S. Chou, M. De, J. Luo, V. M. Rotello, J. Huang and V. P. Dravid, *J. Am. Chem. Soc.*, 2012, **134**, 16725.
7. Q. Liu, J. Shi, J. Sun, W. Thanh, L. Zeng and G. Jiang, *Angew. Chem. Int. Ed.*, 2011, **50**, 6035.
8. C. Wang, S. de Rooy, C.-F. Lu, V. Fernand, L. Moore, Jr., P. Berton and I. M. Warner, *Electrophoresis*, 2013, **34**, 1197.
9. Z. Luo, L. Yuwen, Y. Han, J. Tian, X. Zhu, L. Weng and L. Wang, *Biosens. Bioelectron.*, 2012, **36**, 179.
10. H. Wei, W. Yang, Q. Xi and X. Chen, *Mater. Lett.*, 2012, **82**, 224.
11. S. Guo, S. Dong and E. Wang, *ACS Nano*, 2010, **4**, 547.
12. Y. Ma, L. Sun, W. Huang, L. Zhang, J. Zhao, Q. Fan and W. Huang, *J. Phys. Chem. C,* 2011, **115**, 24592.
13. F. Yavari, Z. Chen, A. V. Thomas, W. Ren, H.-M. Cheng and N. Koratkar, *Sci. Rep-UK*, 2011, **1**, 166.
14. Z.-S. Wu, Y. Sun, Y.-Z. Tan, S. Yang, X. Feng and K. Muellen, *J. Am. Chem. Soc*., 2012, **134**, 19532.
15. Z.-S. Wu, A. Winter, L. Chen, Y. Sun, A. Turchanin, X. Feng and K. Muellen, *Adv. Mater*., 2012, **24**, 5130.
16. A. Bagri, R. Grantab, N. V. Medhekar and V. B. Shenoy, *J. Phys. Chem. C,* 2010, **114**, 12053.
17. Y. Lei, F. Chen, Y. Luo and L. Zhang, *J. Mater. Sci*., 2014, **49**, 4236.
18. F. Liu, S. Chung, G. Oh and T. S. Seo, *ACS Appl. Mater. Interfaces*, 2012, **4**, 922.
19. P. T. Anastas and M. M. Kirchhoff, *Acc. Chem. Res*., 2002, **35**, 686.
20. D. N. Saheb and J. P. Jog, Adv. *Polym. Tech*., 1999, **18**, 351.
21. W. Zhou, H. Chen, Y. Yu, D. Wang, Z. Cui, F. J. DiSalvo and H. D. Abruna, *ACS Nano*, 2013, **7**, 8801.
22. R. Hoover, Carbohydr. Polym., 2001, **45**, 253.
23. R. E. O. William S. Hummers Jr., *J. Am. Chem. Soc*., 1958, **80**, 1339.
24. N. I. Kovtyukhova, P. J. Ollivier, B. R. Martin, T. E. Mallouk, S. A. Chizhik, E. V. Buzaneva and A. D. Gorchinskiy, *Chem. Mater.*, 1999, **11**, 771.
25. S. Stankovich, D. A. Dikin, R. D. Piner, K. A. Kohlhaas, A. Kleinhammes, Y. Jia, Y. Wu, S. T. Nguyen and R. S. Ruoff, *Carbon*, 2007, **45**, 1558.
26. W. Ouyang, J. Sun, J. Memon, C. Wang, J. Geng and Y. Huang, *Carbon*, 2013, **62**, 501.
27. P. Zhu, M. Shen, S. Xiao and D. Zhang, *Physica B-Condensed Matter*, 2011, **406**, 498.
28. L. O. Filippov, V. V. Severov and I. V. Filippova, Int. *J. Miner. Process.*, 2013, **123**, 120.
29. R. K. Rath and S. Subramanian, *Miner. Eng*., 1997, **10**, 1405.
30. J. W. Liu, Q. Zhang, X. W. Chen and J. H. Wang, *Chem. Eur. J*., 2011, **17**, 4864.
31. F. Hook, M. Rodahl, B. Kasemo and P. Brzezinski, *PNAS,* 1998, 95.
32. B.D. Hames, N.M. Hooper, Instant Notes in Biochemistry, Taylor & Francis, UK, 2000, 36.
33. K. K. R. Tetala, K. Skrzypek, M. Levisson and D. F. Stamatialis, *Sep. Purif. Technol.*, 2013, **115**, 20.
34. G. Zhao, S. Chen, X.-W. Chen and R.-H. He, *Anal. Bioanal. Chem*., 2013, **405**, 5353.
35. T. S. Anirudhan and S. R. Rejeena, *Carbohydr. Polym*., 2013, **93**, 518.
36. X. Jia, M. Xu, Y. Wang, D. Ran, S. Yang and M. Zhang, *Analyst*, 2013, **138**, 651.
37. J.-W. Liu, Y. Zhang, X.-W. Chen and J.-H. Wang, *ACS Appl. Mater. Interfaces,* 2014, **6**, 10196.
38. L. Zheng, D. Ye, L. Xiong, J. Xu, K. Tao, Z. Zou, D. Huang, X. Kang, S. Yang and J. Xia, *Anal. Chim. Acta,* 2013, **768**, 69.
39. M. Liu, J. Song, S. Shuang, C. Dong, J. D. Brennan and Y. Li, *ACS Nano*, 2014, **8**, 5564.

Graphical Abstract

A three-dimensional amylopectin-graphene oxide framework (AP-rGO) exhibits excellent adsorption toward hemoglobin with a maximum adsorption capacity of 1010 mg g^{-1}.